

# Conformation of Single Homopolymer Chain in Microphase-Separated Block Copolymer Monolayer Studied by Scanning Near-Field Optical Microscopy

Yasunari Tamai, Ryojun Sekine, Hiroyuki Aoki,\* and Shinzaburo Ito

*Department of Polymer Chemistry, Graduate School of Engineering, Kyoto University, Nishikyo, Kyoto 615-8510, Japan*

*Received February 16, 2009; Revised Manuscript Received May 7, 2009*

**ABSTRACT:** The phase-separated structure of poly(isobutyl methacrylate)-*block*-poly(octadecyl methacrylate) (PiBMA-*b*-PODMA) monolayer and single poly(isobutyl methacrylate) (PiBMA) chain dispersed therein were investigated by scanning near-field optical microscopy (SNOM), which enabled us to observe with high spatial resolution beyond the diffraction limit of light. The conformation of the individual homo-PiBMA chains was quantitatively evaluated from the fluorescence intensity distribution. We found that the homo-PiBMA chains were almost located at the center of the PiBMA domain. The homo-PiBMA chain was oriented itself depending on its location in the PiBMA domain. When the homo-PiBMA chain locates at the center of the PiBMA domain, it tends to orient itself in the direction parallel to the interface between the two microdomains. When the homo-PiBMA chain locates near the interface, it orients itself in the direction perpendicular to the interface.

## Introduction

Block copolymers are known to form microphase-separated structures such as lamellae, cylinders, and spheres, etc.,<sup>1</sup> which have been widely investigated from the viewpoint of the variation of morphology with the composition,<sup>2</sup> the molecular weight dependence of domain size,<sup>3–5</sup> and the chain conformation of a block copolymer chain.<sup>6,7</sup> In the microphase-separated structures, the conformation of the block chain is distorted anisotropically: the block chain is elongated in the direction perpendicular to the interface between the two microdomain, whereas it shrinks in the parallel direction. The mixed system of the block copolymer and the corresponding homopolymers have been of interest. When a homopolymer A dissolves in a block copolymer A-*b*-B, the homopolymer is confined to the A domain formed by A-*b*-B. The location and conformation of the homopolymer chain in the block copolymer lamella have been extensively studied both theoretically<sup>8,9</sup> and experimentally.<sup>10–18</sup> Hasegawa et al. investigated single chain conformation of polystyrene homopolymer dissolved in a lamellar microdomain of polystyrene-*b*-polyisoprene diblock copolymer in bulk by small-angle neutron scattering (SANS).<sup>13</sup> They found that the homopolymer chains with their molecular weights 1 order smaller than that of the block copolymer are extended and contracted in the perpendicular and parallel directions, respectively, similarly to the block chain. On the other hand, Matsushita et al. investigated polystyrene homopolymers with various molecular weights in polystyrene-*b*-poly(2-vinylpyridine) in bulk by SANS.<sup>16</sup> Although the radii of gyration of the homopolymers in the direction perpendicular to the interface were not able to be evaluated due to the experimental difficulty, they found that the homopolymer chains are unperturbed at least in the direction parallel to the interface.

The behavior of the block copolymer in restricted dimensions (e.g., thin film and colloidal particles) differs from that of bulk

system.<sup>18–22</sup> Since the polymer chain in a monolayer is restricted in quasi-two dimensions,<sup>23–26</sup> the monolayer of diblock copolymer can be regarded as a good model system to study the phase separation in a restricted geometry. Previous studies indicated that the polymer chain restricted in such a quasi-two-dimensional plane is not allowed to entangle with the intra- and intermolecular chains and forced to take a contracted conformation.<sup>27–29</sup> Therefore, the phase separation behavior in the two-dimensional system show anomalous features.<sup>21–24,30,31</sup> For example, since the polymer chain has no degree of freedom in the height direction and is not allowed to have crossover on the other chains, the block chain in microphase-separated structures would be expected to be highly elongated in the direction perpendicular to the interface.<sup>21,22</sup> Thus, it is interesting to investigate the features of the mixtures of the block copolymer with the corresponding homopolymers in two-dimensional system; however, it has not been explored due to the lack of suitable experimental techniques.

Characterization of the chain conformations in a bulk medium requires the technique that has both high spatial resolution and the capability to distinguish a single polymer chain from the bulk of the entangled chains. Fluorescence labeling technique is an established method for the selective imaging of such the single chain from its surroundings. However, conventional fluorescence microscopy suffers from the diffraction-limited resolution of a half of the wavelength of the incident light. Therefore, the application of the optical microscopy to single macromolecular imaging has been limited to the observation of huge biomacromolecules such as DNA.<sup>32,33</sup> Scanning near-field optical microscopy (SNOM) has been developed to provide the optical information with the high spatial resolution beyond the diffraction limit of light.<sup>34</sup> SNOM is a scanning probe microscopy technique, which employs the probe tip having an aperture smaller than the wavelength of light. The incident light to the aperture generates an optical near-field restricted in the space of the aperture size, which enables us to illuminate the specimen and to obtain the optical response from the nanometric area.

\*Corresponding author. E-mail: aoki@photo.polym.kyoto-u.ac.jp.

Therefore, the fluorescence imaging by SNOM is a promising technique for the direct observation of a single polymer chain in a bulk medium.<sup>10,29,35,36</sup> Yang et al. investigated the location and orientation of a single homopolymer chain embedded in a block copolymer lamella in the three-dimensional system by using SNOM.<sup>10</sup> A homopolymer with its molecular weight larger than that of a block copolymer tends to locate at the center of corresponding block domain and orient itself depending on its location in the block domain. In this paper, we employ SNOM to observe individual poly(isobutyl methacrylate) (PiBMA) homopolymer chains dispersed in microphase-separated structure of poly(isobutyl methacrylate)-*block*-poly(octadecyl methacrylate) (PiBMA-*b*-PODMA) in two-dimensional monolayer and discuss the conformation of the PiBMA homopolymer chains.

## Experiments

PiBMA-*b*-PODMA was synthesized by the atom transfer radical polymerization.<sup>22</sup> The PiBMA homopolymer randomly labeled by perylene diimide (PDI) (PiBMA:PDI) was synthesized by radical copolymerization of isobutyl methacrylate and PDI-containing methacrylate. The chemical structures are shown in Figure 1. The obtained PiBMA:PDI was purified by the fractional precipitation in methanol from toluene to achieve a relatively narrow molecular weight distribution. The weight- and number-averaged molecular weights,  $M_w$  and  $M_n$ , were

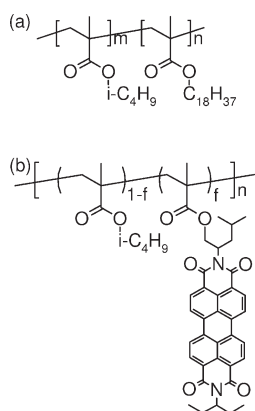


**Figure 1.** Chemical structures of the block copolymer PiBMA-*b*-PODMA (a) and the dye-labeled homopolymer PiBMA:PDI (b).

**Table 1.** Characterizations of PiBMA-*b*-PODMA and PiBMA:PDI

	DP <sub>n</sub> <sup>a</sup> /10 <sup>3</sup>		$M_w/M_n$	$f^b$
	PiBMA	PODMA		
PiBMA- <i>b</i> -PODMA	2.02	1.98	1.10	
PiBMA:PDI	11.0		1.21	0.005

<sup>a</sup> The number-averaged degree of polymerization. <sup>b</sup> The molar fraction of the dye unit.

determined by gel permeation chromatography (D-7000G, Hitachi) with the eluent THF, which was calibrated by PS standards (Scientific Polymer Products) and a PiBMA secondary standard (Aldrich), and <sup>1</sup>H NMR (JNM-EX400, JEOL). The fraction of the dye-labeled unit was evaluated to be 0.5% from UV-vis absorption (U3500, Hitachi). The properties of the PiBMA would not be affected by the introduction of the PDI moiety because of the low dye content. The average distance between the adjacent dye molecules was estimated to be 7.3 nm, which is larger than the Forster radius of the PDI (ca. 4 nm); therefore, the PDI showed monomer-like emission properties. The characterization of these polymers is summarized in Table 1.

The monolayer was prepared by the Langmuir-Blodgett technique. We prepared a mixed solution of the PiBMA-*b*-PODMA and PiBMA:PDI in benzene at a concentration of 0.1 g L<sup>-1</sup>. The fraction of the PiBMA:PDI was 0.25% to PiBMA-*b*-PODMA. The polymer solution was spread on pure water (NANOpure II, Barnstead) at 20 °C. Surface pressure was measured by a Wilhelmy plate. Annealing was carried out by raising the water subphase temperature to 40 °C and keeping it constant for 2 h. Annealing was carried out in a constant area condition without surface pressure control. After cooling the subphase temperature to 20 °C the monolayer was compressed to a surface pressure of 5 mN m<sup>-1</sup> and transferred onto a glass coverslip by the vertical dipping method at a rate of 1.0 mm min<sup>-1</sup>. In order to avoid the fluorescence quenching of the dye moiety, the monolayer was overcoated by a thin layer (10 nm) of poly(vinyl alcohol) (PVA) by the spin-coating method. The SNOM measurement confirmed that the surface morphology of the monolayer was not altered by the overcoating of PVA, and it can be observed through the thin layer of PVA (see Supporting Information).

The SNOM measurement was performed by a commercially available instrument ( $\alpha$ -SNOM, WITec) with a hollow cantilever probe with a subwavelength aperture of 60 nm. The laser beam at a wavelength of 532 nm was focused onto the backside of the aperture to generate the optical near-field. The PDI fluorescence was collected by a microscope objective (0.80 NA, 60 $\times$ , Nikon) from the backside of the substrate and guided to an avalanche photodiode (SPCM-AQR-14, Perkin-Elmer). The SNOM measurement was carried out at contact mode and ambient condition. With our experimental setup, the surface topography (TP) and fluorescence (FL) images can be simultaneously obtained from the scanning area.

## Results and Discussion

Figure 2 shows a set of SNOM images obtained simultaneously from an area of 5  $\mu$ m  $\times$  5  $\mu$ m. The microphase-separated structure of the PiBMA-*b*-PODMA with the regular spacings was clearly observed in the surface topography of Figure 2a. The bright area indicates the higher region than the dark part. Since PODMA has a long alkyl side chain, the thickness of

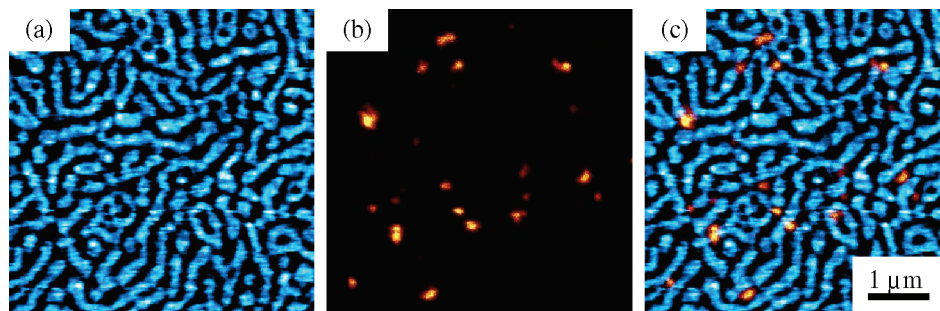


**Figure 2.** SNOM images of the PiBMA-*b*-PODMA/PiBMA:PDI monolayer: (a) surface topography, (b) fluorescence image, and (c) superimposition of the panels (a) and (b). The blue and dark parts in (a) correspond to the PODMA and PiBMA domain, respectively. The bright spot in (b) corresponds to a single PiBMA:PDI chain.

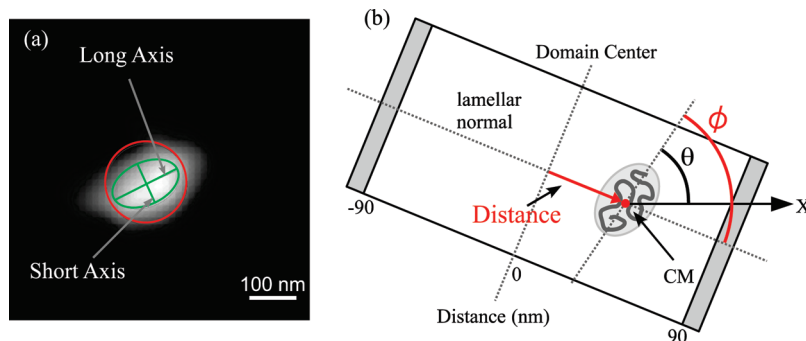


**Figure 3.** (a) Enlarged FL image of a single PiBMA chain. The radius of the red circle is the calculated  $R_{2D}$  of the homo-PiBMA chain. The green ellipse is drawn with the square roots of the two eigenvalues ( $\lambda_l$  and  $\lambda_s$ ) as the long and short axes. The scale bar is 100 nm. (b) Schematic image shows the determination of the distance and orientational angle,  $\phi$ . We set the origin of the distance coordinate to the center of the PiBMA domain and the positive direction to the right-hand side of the image.

the PODMA monolayer is 2 nm thicker than the PiBMA monolayer.<sup>25,26</sup> Therefore, the bright and dark areas in Figure 2a correspond to the PODMA and PiBMA domains, respectively. The FFT pattern of the TP image showed the peak at  $2.9 \mu\text{m}^{-1}$ , indicating that the average width of the PiBMA domain was 180 nm. For a symmetric block copolymer, the most stable phase-separated structure is expected to be a lamellar structure with the parallel orientation. However, partially constructed lamellar structures were observed rather than the long-range ordered lamellar structure as shown in Figure 2a. To obtain a long-range ordered structure, we carried out farther annealing, but little change could be seen after 30 h. On the other hand, in the case of the PiBMA-*b*-PODMA with the low DP of 1600, the long-range ordered lamellar structure was observed within 1 h (the data were not shown here). The rather disordered structure for the high molecular weight PiBMA-*b*-PODMA is explained by both the molecular weight dependence of the surface viscosity<sup>28</sup> and the effect that polymer chains are restricted in the two-dimensional plane. Since overlapping among the polymer chains is not allowed in two dimensions, it is difficult for high molecular weight polymer to rearrange the location and conformation of the polymer chain. Therefore, the long-range ordered lamella cannot be obtained. The bright spot in the FL image of Figure 2b corresponds to the single homo-PiBMA chain dispersed in the block copolymer monolayer.<sup>37</sup> Figure 2c is a superimposed image of the TP and FL images. We can find the bright spot corresponding to the homo-PiBMA chain in the dark area in the TP image. This indicates that the homo-PiBMA chains are located at the PiBMA domain of the microphase-separated structure of the PiBMA-*b*-PODMA lamella.

The conformation of the single PiBMA chain was quantitatively evaluated from the fluorescence intensity distribution.<sup>33</sup> The fluorescence intensity is proportional to the number of fluorescence dye molecules randomly introduced along the PiBMA:PDI main chain; therefore, the intensity at each pixel corresponds to the number of the chain segments therein. The first moment of the fluorescence intensity distribution denotes the position of the center of mass (CM).

$$x_{\text{CM}} = \frac{1}{I_0} \sum_i x_i I_i$$

$$y_{\text{CM}} = \frac{1}{I_0} \sum_i y_i I_i \quad (1)$$

where  $I_i$  is the fluorescence intensity at the  $i$ th pixel,  $(x_i, y_i)$  is the Cartesian coordinate of the  $i$ th pixel, and  $I_0$  is the total

fluorescence intensity from the single chain. The second moment of the fluorescence intensity distribution are expressed as

$$R_{xx}^2 = \frac{1}{I_0} \sum_i (x_i - x_{\text{CM}})^2 I_i$$

$$R_{yy}^2 = \frac{1}{I_0} \sum_i (y_i - y_{\text{CM}})^2 I_i$$

$$R_{xy}^2 = R_{yx}^2 = \frac{1}{I_0} \sum_i (x_i - x_{\text{CM}})(y_i - y_{\text{CM}}) I_i \quad (2)$$

The tensor  $\mathbf{R}$  is a parameter related to the polymer chain conformation.

$$\mathbf{R} = \begin{pmatrix} R_{xx}^2 & R_{xy}^2 \\ R_{yx}^2 & R_{yy}^2 \end{pmatrix} \quad (3)$$

In this way, the investigated polymer chain spot can be represented as an ellipse with long and short principal axes.<sup>32,33</sup> The eigenvalues of the  $\mathbf{R}$ ,  $\lambda_l$ , and  $\lambda_s$  ( $\lambda_l > \lambda_s$ ) are corresponding to the squared lengths of the long and short axes of the most appropriate ellipsoid. The trace of  $\mathbf{R}$  is the square radius of gyration in the  $XY$  plane,  $R_{2D}$ . The angle,  $\theta$ , between the long principal axis and the  $X$ -axis are given by

$$\theta = \arctan \left( \frac{\lambda_l - R_{xx}^2}{R_{xy}^2} \right) \quad (4)$$

Then, the orientational angle,  $\phi$ , of the long principal axis relative to the direction perpendicular to the interface (lamellar normal) was evaluated from the angle,  $\theta$ . Using our methodology of the SNOM image analysis, we analyzed 80 PiBMA:PDI chains located at different areas in the lamellar domains. We summarized the descriptions of these parameters in Figure 3.

The homo-PiBMA chains would show preferred location due to the energetic contribution; therefore, we discuss the distribution of the homo-PiBMA chain in the PiBMA-*b*-PODMA lamellar domains. We estimated the distance between the CM of the homo-PiBMA chain and the center of the PiBMA domain in the direction of the lamellar normal, as shown in Figure 3b. We set the origin of the distance coordinate to the center of the PiBMA domain and the positive direction to the right-hand side of the image. The width of the PiBMA domain was evaluated to be 180 nm as mentioned above; therefore, the interface between the two microdomains correspond to  $\pm 90$  nm in the distance



coordinate. Figure 4 shows the histogram of the distribution of the CM of the homo-PiBMA chains in the PiBMA-*b*-PODMA lamella. It is easily seen that the homo-PiBMA chains are almost localized at the center of the PiBMA domain. In order to discuss the distribution of the homopolymer in the lamellar domain, we fitted the histogram of Figure 4 to a simple hyperbolic tangent form.<sup>8,18</sup>

$$\Psi_h(x) = a \left\{ \tanh\left(\frac{b+2x}{c}\right) + \tanh\left(\frac{b-2x}{c}\right) \right\} \quad (5)$$

where  $a$ ,  $b$ , and  $c$  are the floating parameters used in the fitting. The solid line in Figure 4 indicates the fitting result. The full width at half-maximum (fwhm) was estimated to be 60 nm. Therefore, the ratio of fwhm to the domain width (fwhm/ $D$ ) was evaluated to be 0.33. On the other hand, fwhm/ $D$  of our previous work for a three-dimensional system of polystyrene-*block*-poly(methyl methacrylate)<sup>10</sup> was 0.56 (see Supporting Information). This result indicates that the homopolymer in two dimensions is more concentrated at the domain center compared to the three-dimensional bulk system.

The conformation of the block chains in the microdomain would be different from the unperturbed homopolymer chain.<sup>1,6,7,21,22</sup> Thus, it is interesting to investigate the conformation of the homopolymer chain in the microdomain.<sup>10,13,16</sup> At first, we evaluated the in-plane radius of gyration,  $R_{2D}$ , of the homo-PiBMA chain. The homo-PiBMA chains dispersed in the PiBMA-*b*-PODMA lamella have an average  $R_{2D}$  of  $72 \pm 18$  nm. This value is almost the same as the  $R_{2D}$  of the PiBMA chains in the neat PiBMA monolayer ( $68 \pm 19$  nm).<sup>38</sup>  $R_{2D}$  of the

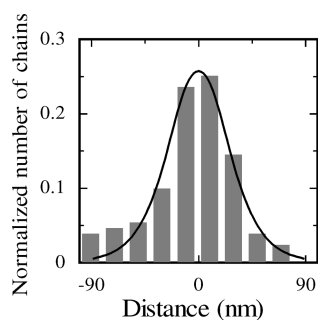


**Figure 4.** Histogram of the distribution of the homo-PiBMA chain in the PiBMA-*b*-PODMA lamellar domain. The normalized population of the homo-PiBMA chains is plotted against the distance between the CM of a homo-PiBMA chain and the center of the PiBMA domain. The interface correspond to  $\pm 90$  nm in the distance coordinate. The solid line indicate the fitted homopolymer distribution.

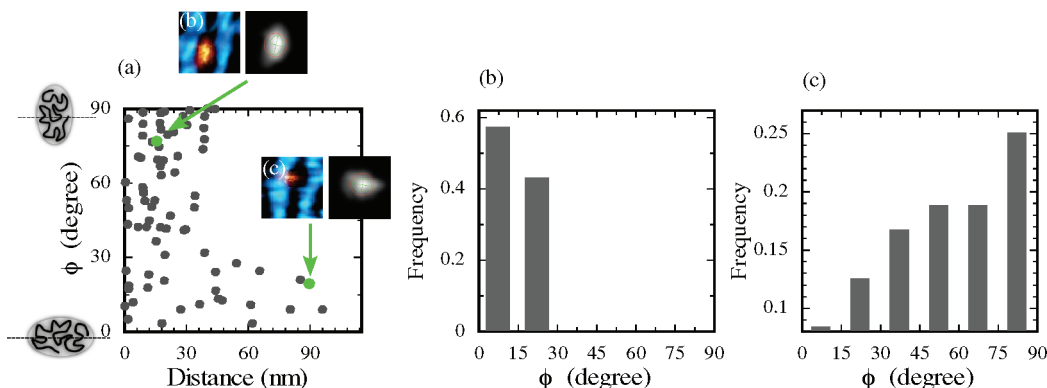


**Figure 5.** Plot of the chain orientation of the homo-PiBMA chains against the CM location in the PiBMA domain (a) and histograms of the angle,  $\phi$ , of the homo-PiBMA located near the interface (b) and at the center of the PiBMA domain (c). X-axis in panel (a) shows the absolute value of the distance between the CM of a homo-PiBMA chain and the center of the PiBMA domain. Each point indicate a single PiBMA chain.

homopolymer is not significantly altered in the microphase-separated structure. Now we discuss the conformational orientation of the PiBMA chain embedded in the lamellar domain. The orientational angle,  $\phi$ , between the long axis of the ellipsoid and the lamellar normal for each individual homo-PiBMA chain was plotted against the absolute distance in the lamellar domain in Figure 5a. We found that the homo-PiBMA chains showed the orientation depending on the location of the homo-PiBMA chain in the PiBMA domain.<sup>39</sup> Most of the PiBMA chains at the location of  $>60$  nm showed the orientational angle of  $<30^\circ$ . Figure 5b shows the histogram of the orientational angle at distance of  $>60$  nm. Figure 5b clearly indicates that the homo-PiBMA chain has the preferential orientation in the direction perpendicular to the interface. On the other hand, around the center of the lamellar domain, it seems that the chain orientation shows random distribution. Figure 5c shows the histogram of the orientational angle for the chains located at the domain center (distance  $<25$  nm), indicating that the homo-PiBMA chain shows weak tendency to orient itself parallel to the interface. In Figure 5a, we also show the superimposed (TP and FL) images of two homo-PiBMA chains located at different positions in the PiBMA domain. From these images, one can easily see the tendency of the conformational orientation dependence on the location in the PiBMA domain.

A schematic image of the homo-PiBMA chain orientation in the PiBMA-*b*-PODMA lamella is shown in Figure 6. It is well-known that the structure of a phase-separated block copolymer system is determined by the balance of the enthalpic gain by the separation of the incompatible block chains and the loss of the entropy due to the restricted conformation at the interface. When an ordered structure is formed, the block chains takes a brushlike conformation with the loss of the conformational entropy so as to reduce the unfavorable contact.<sup>1,6,7</sup> Especially, in the case of the two-dimensional system, since the polymer chains not be allowed to have crossover with the other chains, the block chains would have to take highly stretched conformation in the direction perpendicular to the interface.<sup>21,22</sup> If the homo-PiBMA chain is sparsely located in a matrix of the PiBMA-*b*-PODMA lamella, the individual chain is confined to the PiBMA domain due to the repulsive interaction with PODMA. Since the investigated homo-PiBMA chain has a relatively large molecular weight, it occupies a large area in the monolayer. If the homo-PiBMA chain existed in the copolymer brushes, it would disturb the brush conformation, resulting in the large entropic loss for the block chain. Therefore, the homo-PiBMA chain is expected to be excluded from the brushes and localized in the center of the PiBMA domain with narrower distribution than three-dimensional system due to the no degree of the crossover and entanglement.

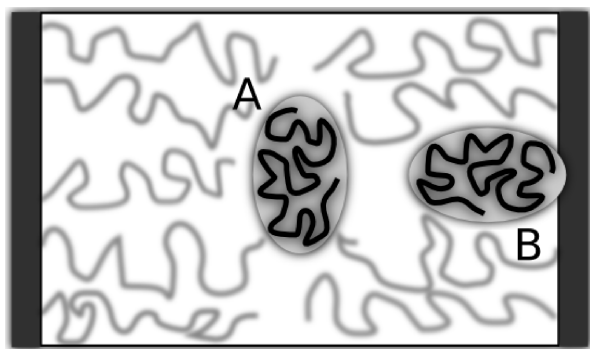


**Figure 6.** Schematic image of the relationship between the orientation and location of the homo-PiBMA chains. The gray coils represent the PiBMA block chains. The black coils and elliptical shadow represent homo-PiBMA chains.

The homo-PiBMA chain is anisotropically confined by the brushes. The homo-PiBMA chain located at the center of the PiBMA domain is restricted not to expand in the direction perpendicular to the interface due to the no degree of the cross-over and entanglement with the brushes. Consequently, the homo-PiBMA chain were contracted in the direction perpendicular to the interface and extended in the parallel direction as shown in chain A in Figure 6. On the other hand, some homo-PiBMA chains were located near the interface and showed elongated conformations perpendicular to the interface as shown in chain B in Figure 6. The homopolymer chain located near the interface would take a conformation along the block chain, which takes a stretched conformation perpendicular to the interface not to distort the brush conformation. A similar result was reported in our previous work for a three-dimensional system.<sup>10</sup> While only a weak tendency could be seen for the three-dimensional system (see Supporting Information), we found a strong correlation between the location and orientation of a homo-PiBMA chain in the two-dimensional system. Almost all the homo-PiBMA chains located near the interface orient themselves in the direction perpendicular to the interface (Figure 5b). This is due to the confinement effect in two dimensions. Since the crossover and entanglement among the polymer chain are not allowed in two dimensions, the homopolymer chain dispersed in the microphase-separated monolayer is strongly affected by the block chain organization.

## Conclusion

The phase-separated structure of poly(isobutyl methacrylate)-*block*-poly(octadecyl methacrylate) (PiBMA-*b*-PODMA) monolayer and single poly(isobutyl methacrylate) (PiBMA) chain dispersed therein were investigated by SNOM. We could directly observe the individual dye-labeled PiBMA chains dispersed in the microphase-separated block copolymer monolayer by SNOM. We found that the homo-PiBMA chains were almost located at the center of the PiBMA domain. The homopolymer chain was oriented itself depending on its location in the block domain. When the homo-PiBMA chain locates at the center of the PiBMA domain, it tends to orient itself in the direction parallel to the interface. When the homo-PiBMA chain locates near the interface, it orient itself in the direction perpendicular to the interface. This is because the effect of the anisotropic confinement from the block chain organization.

**Acknowledgment.** This work was supported by Grants-in-Aid from Japan Society for the Promotion of Science (JSPS) and Ministry of Education, Culture, Sports, Science and Technology (MEXT), Japan. The authors also acknowledge the Innovative Techno-Hub for Integrated MedicalBio-imaging Project of the

Special Coordination Funds for Promoting Science and Technology from MEXT.

**Supporting Information Available:** Descriptions of experiments on distinguishing PiBMA and PODMA domains in the PiBMA-*b*-PODMA monolayer and results on the homopolymer distribution and the distributions of the orientational angle in a three-dimensional system. This material is available free of charge via the Internet at <http://pubs.acs.org>.

## References and Notes

- (1) Bates, F. S.; Fredrickson, G. H. *Annu. Rev. Phys. Chem.* **1990**, *41*, 525–557.
- (2) Inoue, T.; Soen, T.; Hashimoto, T.; Kawai, H. *J. Polym. Sci., Part A2* **1969**, *7*, 1283–1301.
- (3) Helfand, E.; Wasserman, Z. R. *Macromolecules* **1976**, *9*, 879–888.
- (4) Hashimoto, T.; Shibayama, M.; Kawai, H. *Macromolecules* **1980**, *13*, 1237–1247.
- (5) Matsushita, Y.; Mori, K.; Saguchi, R.; Nakao, Y.; Noda, I.; Nagasawa, M. *Macromolecules* **1990**, *23*, 4313–4316.
- (6) Hasegawa, H.; Hashimoto, T.; Kawai, H.; Lodge, T. P.; Amis, E. J.; Glinka, C. J.; Han, C. C. *Macromolecules* **1985**, *18*, 67–78.
- (7) Matsushita, Y.; Mori, K.; Mogi, Y.; Saguchi, R.; Noda, I.; Nagasawa, M.; Chang, T.; Glinka, C. J.; Han, C. C. *Macromolecules* **1990**, *23*, 4317–4321.
- (8) Shull, K. R.; Winey, K. I. *Macromolecules* **1992**, *25*, 2637–2644.
- (9) Vavasour, J. D.; Whitmore, M. D. *Macromolecules* **2001**, *34*, 3471–3483.
- (10) Yang, J.; Sekine, R.; Aoki, H.; Ito, S. *Macromolecules* **2007**, *40*, 7573–7580.
- (11) Hashimoto, T.; Tanaka, H.; Hasegawa, H. *Macromolecules* **1990**, *23*, 4378–4386.
- (12) Tanaka, H.; Hasegawa, H.; Hashimoto, T. *Macromolecules* **1991**, *24*, 240–251.
- (13) Hasegawa, H.; Tanaka, H.; Hashimoto, T.; Han, C. C. *J. Appl. Crystallogr.* **1991**, *24*, 672–678.
- (14) Koizumi, S.; Hasegawa, H.; Hashimoto, T. *Macromolecules* **1994**, *27*, 7893–7906.
- (15) Matsushita, Y.; Torikai, N.; Mogi, Y.; Noda, I.; Han, C. C. *Macromolecules* **1993**, *26*, 6346–6349.
- (16) Matsushita, Y.; Torikai, N.; Mogi, Y.; Noda, I.; Han, C. C. *Macromolecules* **1994**, *27*, 4566–4569.
- (17) Torikai, N.; Takabayashi, N.; Noda, I.; Koizumi, S.; Morii, Y.; Matsushita, Y. *Macromolecules* **1997**, *30*, 5698–5703.
- (18) Mayes, A. M.; Russell, T. P.; Satija, S. K.; Majkrzak, C. F. *Macromolecules* **1992**, *25*, 6523–6531.
- (19) Orso, K. A.; Green, P. F. *Macromolecules* **1999**, *32*, 1087–1092.
- (20) Okubo, M.; Saito, N.; Takekoh, R.; Kobayashi, H. *Polymer* **2005**, *46*, 1151–1156.
- (21) Kumaki, J.; Hashimoto, T. *J. Am. Chem. Soc.* **1998**, *120*, 423–424.
- (22) Aoki, H.; Kunai, Y.; Ito, S.; Yamada, H.; Matsushige, K. *Appl. Surf. Sci.* **2002**, *188*, 534–538.
- (23) Gabrielli, G.; Puggelli, M.; Baglioni, P. *J. Colloid Interface Sci.* **1982**, *86*, 485–500.
- (24) Wu, S.; Huntsber Jr. *J. Colloid Interface Sci.* **1969**, *29*, 138–147.
- (25) Naito, K. *J. Colloid Interface Sci.* **1989**, *131*, 218–225.
- (26) Mumby, S. J.; Swalen, J. D.; Rabolt, J. F. *Macromolecules* **1986**, *19*, 1054–1059.
- (27) de Gennes, P. G. *Scaling Concepts in Polymer Physics*; Cornell University Press: Ithaca, NY, 1979.
- (28) Sato, N.; Ito, S.; Yamamoto, M. *Macromolecules* **1998**, *31*, 2673–2675.
- (29) Aoki, H.; Anryu, M.; Ito, S. *Polymer* **2005**, *46*, 5896–5902.
- (30) Aoki, H.; Sakurai, Y.; Ito, S.; Nakagawa, T. *J. Phys. Chem. B* **1999**, *103*, 10553–10556.
- (31) Aoki, H.; Ito, S. *J. Phys. Chem. B* **2001**, *105*, 4558–4564.
- (32) Maier, B.; Radler, J. O. *Phys. Rev. Lett.* **1999**, *82*, 1911–1914.
- (33) Maier, B.; Radler, J. O. *Macromolecules* **2001**, *34*, 5723–5724.
- (34) Betzig, E.; Trautman, J. K. *Science* **1992**, *257*, 189–195.
- (35) Ube, T.; Aoki, H.; Ito, S.; Horinaka, J.; Takigawa, T. *Polymer* **2007**, *48*, 6221–6225.
- (36) Aoki, H.; Morita, S.; Sekine, R.; Ito, S. *Polymer J.* **2008**, *40*, 274–280.
- (37) We blended the PiBMA-*b*-PODMA with different trace amounts of the PiBMA:PDI and measured by SNOM for each sample.

The FL images show that all fluorescent spots are homogeneously distributed throughout the monolayer. For each FL image, we calculated the number density of the fluorescence spots. The number density of the fluorescent spots is in good agreement with the number density of the PiBMA:PDI chains in the PiBMA-*b*-PODMA, based on the molar ratio. This indicates that homo-PiBMA chains did not aggregate and one fluorescent spot in the FL images corresponds to a single PiBMA:PDI chain dispersed in the PiBMA-*b*-PODMA.

- (38) We estimated  $R_g$  of the homo-PiBMA chains dispersed in the PiBMA monolayer matrix by the same method mentioned above. The  $DP_n$  of the matrix PiBMA is 2200, which is almost the same as the  $DP_n$  of the PiBMA block of the PiBMA-*b*-PODMA.
- (39) We also estimated the orientational angle of the homo-PiBMA chains in the neat PiBMA monolayer. We followed the same method mentioned above. FL images show that the homo-PiBMA chains have no preferred orientation in the PiBMA monolayer matrix.